

ORIGINAL ARTICLE

Control of Glutamate Transport by Extracellular Potassium: Basis for a Negative Feedback on Synaptic Transmission

Theresa S. Rimmele^{1,†}, Anne-Bérengrère Rocher^{1,†}, Joel Wellbourne-Wood¹ and Jean-Yves Chatton^{1,2}

¹Department of Fundamental Neurosciences, University of Lausanne, CH-1005 Lausanne, Switzerland and

²Cellular Imaging Facility, University of Lausanne, CH-1005 Lausanne, Switzerland

Address correspondence to Jean-Yves Chatton, Department of Fundamental Neurosciences, University of Lausanne, Rue Bugnon 9, CH-1005 Lausanne, Switzerland. Email: jean-yves.chatton@unil.ch

[†]Co-first authors.

Abstract

Glutamate and K^+ , both released during neuronal firing, need to be tightly regulated to ensure accurate synaptic transmission. Extracellular glutamate and K^+ ($[K^+]_o$) are rapidly taken up by glutamate transporters and K^+ -transporters or channels, respectively. Glutamate transport includes the exchange of one glutamate, 3 Na^+ , and one proton, in exchange for one K^+ . This K^+ efflux allows the glutamate binding site to reorient in the outwardly facing position and start a new transport cycle. Here, we demonstrate the sensitivity of the transport process to $[K^+]_o$ changes. Increasing $[K^+]_o$ over the physiological range had an immediate and reversible inhibitory action on glutamate transporters. This K^+ -dependent transporter inhibition was revealed using microspectrofluorimetry in primary astrocytes, and whole-cell patch-clamp in acute brain slices and HEK293 cells expressing glutamate transporters. Previous studies demonstrated that pharmacological inhibition of glutamate transporters decreases neuronal transmission via extrasynaptic glutamate spillover and subsequent activation of metabotropic glutamate receptors (mGluRs). Here, we demonstrate that increasing $[K^+]_o$ also causes a decrease in neuronal mEPSC frequency, which is prevented by group II mGluR inhibition. These findings highlight a novel, previously unreported physiological negative feedback mechanism in which $[K^+]_o$ elevations inhibit glutamate transporters, unveiling a new mechanism for activity-dependent modulation of synaptic activity.

Key words: astrocyte, electrophysiology, metabotropic glutamate receptors, sodium imaging

Introduction

Glutamate, which is released in the synaptic cleft during neuronal activity, is the predominant excitatory neurotransmitter in the mammalian CNS. Extracellular glutamate is taken up against its concentration gradient by excitatory amino-acid transporters such as GLAST and GLT-1. These transporters are mainly expressed at the astrocytic (Rothstein et al. 1994) and, to a lesser degree, at the neuronal membranes (Rimmele and

Rosenberg 2016). Fast removal of glutamate from the synaptic cleft is pivotal for signal transmission accuracy and prevention of over-excitation. To date, the modulation of glutamate uptake on excitatory neurotransmission has been studied in regards to changes in astrocytic coverage (Oliet et al. 2001), and action of pharmacological inhibitors (Maki et al. 1994; Iserhot et al. 2004; Tsukada et al. 2005). Here, however, we evidenced and characterized physiological modulation of glutamate transport itself.

Glutamate transport is driven by the inwardly directed Na⁺ gradient across the plasma membrane (Levy et al. 1998; Danbolt 2001). Transporting one glutamate into the cell is electrogenic as it is accompanied by the uptake of 3 Na⁺ and one H⁺, and by the extrusion of one K⁺ (Brew and Attwell 1987; Szatkowski et al. 1990; Barbour et al. 1994; Zerangue and Kavanaugh 1996; Bergles and Jahr 1997; Levy et al. 1998). This release of K⁺ is proposed to be compulsory for the glutamate transporter to start a new uptake cycle (Kanner 2006). Transporters of other neurotransmitters such as GABA or homologs of glutamate transporters from prokaryotes do not share this K⁺ component (Slotboom et al. 1999; Kanner 2006).

During neuronal activity, K⁺ is released from repolarizing neurons, as well as extruded from AMPA and NMDA receptors (AMPA, NMDAR) at the synaptic cleft (Shih et al. 2013). While the resting extracellular K⁺ concentration ([K⁺]_o) is around 3 mM, during intense activity [K⁺]_o increases and can reach ~12 mM (Kofuji and Newman 2004). Even higher concentrations are reached in pathological situations such as spreading depression. Glutamate and K⁺ regulation, which are pivotal astrocytic functions, have so far only been studied separately or under non-physiological conditions, e.g., 30–60 mM [K⁺]_o (Rossi et al. 2000). One glutamate taken up by glutamate transporter is linked to the efflux of one K⁺ into the extracellular space at the time K⁺ needs to be cleared out of the extracellular space. Thus, the 2 functions work against each other regarding K⁺ movements.

The aim of this study was to investigate the cross-talk between glutamate transport and [K⁺]_o, and its functional consequences. In particular, we investigated the impact of altered [K⁺]_o on glutamate transporter activity, monitored in primary astrocytes, HEK293 cells expressing GLT-1, and in astrocytes of mouse acute cortical slices. We then evaluated the functional outcome of these interactions on neuronal function in acute cortical slices. We demonstrate for the first time that [K⁺]_o exerts tight control over the kinetics of the glutamate transporter. A moderate increase in [K⁺]_o, as observed in physiological conditions, scales down glutamate uptake. This reduced glutamate clearance decreases neurotransmission notably through activation of mGluRs, inhibiting presynaptic glutamate release. These findings reveal a novel negative feedback cascade linking [K⁺]_o elevation, glutamate transporter inhibition, and presynaptic mGluR activation, which together provide the basis for a previously unseen activity-dependent neuromodulatory mechanism.

Material and Methods

Animals

All experimental procedures were approved by the Veterinary Affairs Office of the Canton of Vaud, Switzerland (authorization number 1288.5-6) and were conducted in strict accordance with the animal care guidelines outlined in the Swiss Ordinance on Animal Experimentation in order to minimize the number and suffering of animals used in all experiments of this study.

Cell Culture

Cortical astrocytes in primary culture were prepared from 1- to 3-days-old C57BL/6 mice as described elsewhere (Sorg and Magistretti 1992). Astrocytes were plated on coverslips and cultured for 3–4 weeks in DME medium (DMEM) plus 10% FCS before experiments. HEK293 cells stably expressing GLT-1 (HEK-GLT-1) were also cultured in DMEM, and plated on coverslips the day before experiments.

Fluorescence Imaging and Astrocyte Transfection

Low-light level fluorescence imaging was performed on an inverted epifluorescence microscope (Axiovert 100 M, Carl Zeiss) using a 40×1.3 N.A. oil-immersion objective lens. Fluorescence excitation wavelengths were selected using a monochromator (Till Photonics) and fluorescence was detected using a 12-bit cooled CCD camera (Princeton Instruments) or EM-CCD camera (Andor). Image acquisition was computer-controlled using Metafluor software (Molecular Devices). Dye-loaded cells were placed in a thermostated chamber designed for rapid exchange of perfusion solutions (Chatton et al. 2000) and superfused at 35 °C.

Experimental solutions contained (mM) NaCl, 135; KCl, 5.4; NaHCO₃, 25; CaCl₂, 1.3; MgSO₄, 0.8; and NaH₂PO₄, 0.78, glucose, 5, bubbled with 5% CO₂/95% air. Bicarbonate-free HEPES-solutions contained (mM) NaCl, 160; KCl, 5.4; HEPES, 20; CaCl₂, 1.3; MgSO₄, 0.8; NaH₂PO₄, 0.78; glucose, 5; bubbled with air. When using different K⁺ concentrations (3–15 mM), NaCl was adjusted to maintain isotonicity. Solutions for dye loading contained (mM) NaCl, 160; KCl, 5.4; HEPES, 20; CaCl₂, 1.3; MgSO₄, 0.8; NaH₂PO₄, 0.78; glucose, 20 and were supplemented with 0.1% Pluronic F-127 (Molecular Probes). In experiments involving more than one solution application, the order was alternated between experiments in order to exclude order-related effects.

For Na⁺ imaging experiments, astrocytes were loaded at 37 °C for 40 min with the Na⁺-sensitive indicator Asante Natrium Green-1 acetoxymethyl ester (ANG-1, 10 μM, TEFLabs) (Lamy and Chatton 2011). ANG-1 fluorescence was excited at 515 nm and detected at 535–585 nm. For in situ calibration, cells were permeabilized for monovalent cations using 10 μg/ml monensin, 3 μg/ml gramicidin with simultaneous inhibition of the Na⁺/K⁺-ATPase by 1 mM ouabain as described earlier (Chatton et al. 2000). This ouabain concentration causes maximal inhibition of Na⁺/K⁺-ATPase. Cells were then sequentially perfused with solutions buffered at pH 7.2 with 20 mM HEPES and containing 0, 5, 10, 20, 50, 100 mM Na⁺, respectively, and 30 mM Cl⁻, 135 mM gluconate with a constant total concentration of Na⁺ and K⁺ of 160 mM. Experiments using Sodium binding benzofuran isophthalate-acetoxymethyl ester (SBFI, Teflabs) were performed as described before (Chatton et al. 2000).

Intracellular Mg²⁺ was monitored using the fluorescent probe Magnesium Green-AM (MgG, Invitrogen), loaded at 37 °C for 20 min with 14 μM dye. MgG fluorescence was imaged as previously described (Magistretti and Chatton 2005).

For intracellular ATP level measurements, astrocytes were treated with 3/2 ratio of Lipofectamine (Life Technologies) and DNA encoding for FRET sensor AT1.03 (ATeam cyto, Imamura et al. 2009). After 4 h, the medium was changed with DMEM plus 10% FCS and cells were used for experiments 2 days after transfection.

Acute Brain Slice Preparation and Electrophysiological Recordings

Experiments were performed on layer II/III neocortical astrocytes in acute slices obtained from 3 week-old C57BL/6 mice. After decapitation and brain extraction, 250 μm-thick coronal slices were prepared with a vibratome (VT 1000 S, Leica). For astrocyte recordings, slices were incubated with an astrocyte-specific dye, sulforhodamine 101 (SR101, 1 μM, 20 min at 32 °C) before being transferred to the recording chamber. Slices were then held down by a platinum harp and superfused by oxygenated 32 °C artificial cerebrospinal fluid (ACSF). Recording

chamber was attached to a Zeiss LSM510 Meta upright microscope equipped with infrared-differential interference contrast and allowing for visualization of SR101-labeled cells. Astroglial cells were selected in layer II/III by their small soma size (<10 μm) and SR101 staining, and then recorded in whole-cell configuration. They were identified by their linear current-voltage (I - V) relationship, the lack of action potentials, and their characteristic negative resting potential (-77.8 ± 0.6 mV). External ACSF solution contained (in mM): NaCl 125, KCl 3, NaHCO_3 26, CaCl_2 2, MgCl_2 2, NaH_2PO_4 1.25, glucose 10 and bubbled with 95% O_2 , 5% CO_2 .

Whole-cell patch-clamp was obtained with borosilicate glass pipettes (>8 M Ω , 4–6 M Ω and 5–7 M Ω resistance for layer III neurons, astrocytes, and HEK-GLT-1 cells, respectively). The patch-clamp intracellular solution contained (in mM): K-gluconate 124, NaCl 6, KCl 6, MgCl_2 3, EGTA 1, CaCl_2 0.5, HEPES 10, glutathione 2, Mg-ATP 3, and Na_3 -GTP 0.3 for astrocytes and K-gluconate 120, NaCl 5, KCl 5, MgCl_2 1, EGTA 0.1, CaCl_2 0.025, HEPES 10, glucose 4, Mg-ATP 1, and Na_3 -GTP 0.2 for neurons (pH 7.3 with KOH, 290 mOsm). Recordings were obtained in voltage-clamp configuration using a Multiclamp 700B amplifier (Molecular Devices) in gap-free mode with a holding potential set at -80 mV. Data were acquired at 10 kHz and filtered at 2 kHz by a Digidata 1440 analog-to-digital converter, controlled with the pCLAMP 10 software. Criteria for experiment inclusion in data analysis were based on the verification of stable access resistance and stable injected current (≤ 100 pA at -80 mV in 3 mM K^+ solution).

During electrophysiological experiments for assessment of the glial glutamate uptake in acute brain slices, D-AP5 (50 μM) was applied 5 min before the onset of recordings and throughout the experiment. External solutions of 3 mM, 5.4 mM, and 8 mM K^+ were sequentially superfused in randomized order over HEK-GLT-1 cells or acute slices. For each of these conditions, and after the measured current stabilized, the same solution with either 200 μM glutamate (HEK-GLT-1 cells) or 1 mM D-aspartate (D-Asp, acute brain slices) was delivered in the bath until maximal response was observed.

To measure the effect of increased $[\text{K}^+]_o$ on the excitatory neurotransmission in acute brain slices, we recorded mini-excitatory post-synaptic currents and potentials (mEPSCs and mEPSPs) from layer II/III neurons in the whole-cell patch-clamp configuration in 3 versus 6 mM K^+ . Recordings were performed in presence of tetrodotoxin (TTX, 1 μM) and bicuculline (60 μM) to block Na_v channels and spiking activity, and GABAergic neurotransmission, respectively. The holding potential for mEPSC recordings was -80 mV. No current was injected for mEPSP recording, allowing the membrane potentials of cells to vary upon different $[\text{K}^+]_o$ applications. For mEPSC/P recordings, each condition was monitored for 10 minutes and the last 2 were analyzed. Cells included in the analysis had a membrane potential < -55 mV or < 150 pA of current injected for a voltage held at -70 mV, stable access resistance, and recovery after washout. mEPSCs were primarily mediated by non-NMDA glutamate receptor activation, as they were blocked by application of the non-NMDA glutamate receptor antagonist CNQX (10 μM), but not by the application of the NMDAR antagonist D-AP5 (50 μM) nor the presence of the GABAR antagonist bicuculline (60 μM , data not shown).

Data Analysis and Statistics

Fluorescence intensity traces were drawn from up to 10 individual cells from the field of view. Current amplitude

measurements were assessed using Clampfit (Molecular Devices). mEPSCs median amplitudes and mean frequencies were measured after automatic detection followed by manual editing of the events in MiniAnalysis (Synaptosoft) for baseline, test condition(s), and washout. Further calculations were done with Excel (Microsoft). Graphs, curve fitting, and statistical analyses were done using KaleidaGraph (Synergy Software). Unless otherwise indicated, a 1-way ANOVA was performed for each experimental group to assess the statistical significance against respective controls, *, **, and *** refer to P values lower than 0.05, 0.01, and 0.001, respectively.

Drugs

D-AP5 was obtained from Biotrend, TTX, SNX482, and ω -Agatoxin-TK from Alomone Labs and bicuculline, (2S, 3S)-3-[3-[4-(trifluoromethyl)benzoylamino]benzyloxy]aspartate (TFB-TBOA) and LY341495 from Tocris Bioscience. All other chemicals were from Sigma-Aldrich.

Results

$[\text{K}^+]_o$ Influences Glutamate Transporter Responses

Glutamate transporter activity was dynamically monitored by measuring the $[\text{Na}^+]_i$ changes associated with transport activity (Chatton et al. 2000) using the sodium sensitive dye Asante Natrium Green-1 (ANG-1) (Lamy and Chatton 2011). Virtually all cells responded to glutamate application with a rapid and reversible increase in $[\text{Na}^+]_i$ as previously observed (Rose and Ransom 1996b; Chatton et al. 2000; Lamy and Chatton 2011). ANG-1-loaded astrocytes were superfused with various $[\text{K}^+]_o$ concentrations spanning the described extracellular concentration range found in vivo during physiological and pathological activity, namely 3, 5.4, 8, 10 and 15 mM, and ANG-1 signal was imaged (Fig. 1A). After a stable baseline was achieved in each $[\text{K}^+]_o$ condition, glutamate (200 μM) was applied. Figure 1A depicts representative cell responses to glutamate application in 5.4 and 15 mM $[\text{K}^+]_o$. As seen on the trace, resting $[\text{Na}^+]_i$ levels were modulated by $[\text{K}^+]_o$ (Fig. 1B). Increasing $[\text{K}^+]_o$ from 3 to 15 mM monotonically decreased baseline $[\text{Na}^+]_i$ from 14.71 ± 1.15 to 5.54 ± 0.60 mM (Fig. 1C). These findings are consistent with previous reports on $[\text{Na}^+]_i$ homeostasis revealing the involvement of Na,K-ATPase and Na,K,Cl cotransporter (NKCC) (Rose and Ransom 1996a; Bittner et al. 2011). As described previously using SBFI, another Na^+ sensitive indicator (Chatton et al. 2000), glutamate application also caused a rapid rise of $[\text{Na}^+]_i$ that returned to baseline after washout of glutamate (Fig. 1B). The amplitude of the glutamate-induced Na^+ response was increased by 12% in low $[\text{K}^+]_o$ (3 mM) compared to the amplitude recorded at 5.4 mM $[\text{K}^+]_o$. Conversely, high $[\text{K}^+]_o$ decreased the response by more than 65% (Fig. 1B, D). Analysis of the initial linear rate of $[\text{Na}^+]_i$ rise (i.e., first 10–20 s) (Fig. 1E) showed that glutamate in low $[\text{K}^+]_o$ evoked an almost 2-fold faster increase in $[\text{Na}^+]_i$ (24.30 ± 1.56 mM \cdot min $^{-1}$) compared to the response in high $[\text{K}^+]_o$ (13.62 ± 0.94 mM \cdot min $^{-1}$). Control experiments performed using the ratiometric Na^+ -sensitive probe SBFI yielded the same results, indicating that the observed effects are not attributable to a $[\text{K}^+]_o$ -induced swelling of astrocytes (see Supplementary Fig. S1). These results show that $[\text{K}^+]_o$ fluctuations have a strong impact on the glutamate-induced Na^+ response in astrocytes.

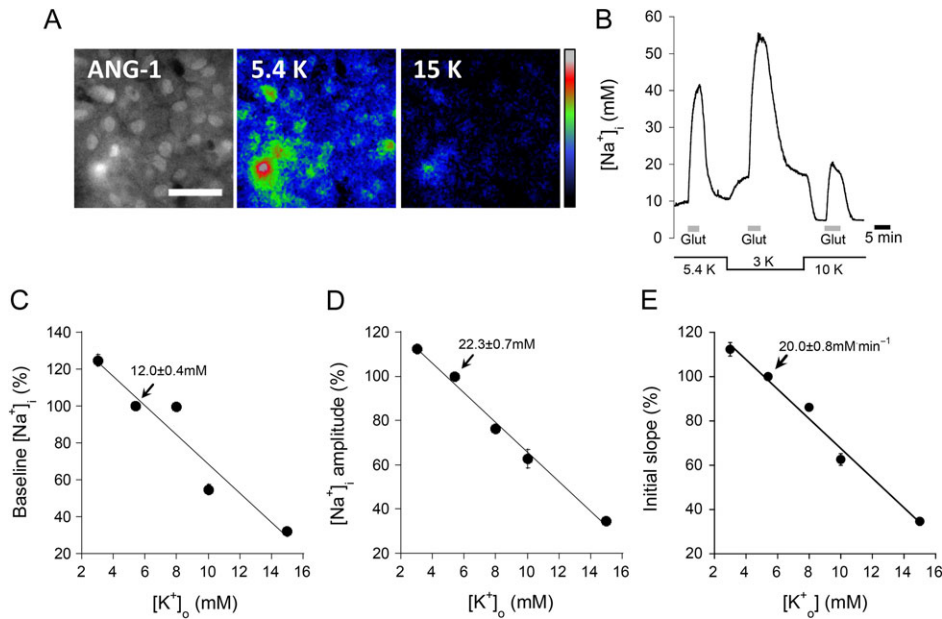


Figure 1. $[K^+]_o$ influences the $[Na^+]_i$ response to glutamate. (A) Images of ANG-1-loaded astrocytes shown in gray scale (left) and in color coded amplitude of fluorescence change observed for glutamate application in 5.4 (middle) and 15 mM (right) $[K^+]_o$. Scale bar: 50 μ m. (B) Single-cell representative trace of $[Na^+]_i$ responses to 200 μ M glutamate superfusion in 3, 5.4 and 10 mM $[K^+]_o$. The $[Na^+]_i$ response to glutamate was modulated by the level of $[K^+]_o$. Mean values of (C) baseline, (D) amplitude, and (E) initial slope were normalized to the value measured at 5.4 mM $[K^+]_o$ and plotted against $[K^+]_o$ ($n = 168$ cells, 17 exp) and showed a linear relationship.

Acute Effects of $[K^+]_o$ on the Na^+ Response to Glutamate

We next investigated whether the observed $[K^+]_o$ modulation of glutamate transport required the establishment of a steady-state K^+ -gradient across the plasma membrane. We compared glutamate response under different conditions (Fig. 2A): glutamate application in 3 mM $[K^+]_o$ steady-state conditions versus acute applications of glutamate and 3 mM $[K^+]_o$. Here, where cells were not allowed time to adjust intracellular cation levels, the amplitude of $[Na^+]_i$ response was further enhanced compared to the control condition with steady-state baseline $[K^+]_o$. It even almost doubled the response amplitude observed in 5.4 mM $[K^+]_o$ (Fig. 2B). The analysis of the initial rate of $[Na^+]_i$ rise (Fig. 2C) showed the same trend for glutamate application in low $[K^+]_o$ in both acute and steady-state conditions. Extended to higher $[K^+]_o$ concentrations, this analysis revealed that the inhibitory effects of $[K^+]_o$ are also more marked for synchronized applications (Fig. 2D,E). Thus, the effects of $[K^+]_o$ on glutamate transport are compatible with a direct and immediate action on the glutamate-induced response. They also indicate that synchronized glutamate and $[K^+]_o$ application, closer mimicking the in situ situation, leads to steeper and more pronounced effects. The involvement of the glutamate transporter as the direct target of K^+ -modulation was confirmed by using D-Asp, a non-metabolized substrate of the glutamate transporters that does not activate non-NMDAR, which yielded a similar trend in amplitude, initial slope, and potentiation in acute application as they did with glutamate (see Supplementary Fig. S2).

$[K^+]_o$ Effects are not Mediated by Intracellular pH Changes

$[K^+]_o$ elevations are known to cause an alkalization of astrocyte cytosol that is mediated by the electrogenic bicarbonate transporter NBCe1 (Deitmer and Rose 1996; Schmitt et al. 2000; Chesler 2003; Ruminot et al. 2011). Depolarization causes this transporter to operate in reverse mode leading to HCO_3^- influx

and alkalization. To exclude that pH changes mediate the observed $[K^+]_o$ modulation, CO_2/HCO_3^- -buffered salines were replaced by HEPES-buffered salines in which no intracellular pH change was found to occur upon switching $[K^+]_o$ (data not shown). Supplementary Figure S3 shows that the effects of $[K^+]_o$ closely match those found in the presence of HCO_3^- . These experiments indicate that cellular alkalization is not the key mediator of the $[K^+]_o$ effect on the response to glutamate.

$[K^+]_o$ Modulates the Kinetics of the Glutamate Transporter

Since glutamate transporters and the Na,K-ATPase both contribute to the shaping of the Na^+ response to glutamate (Chatton et al. 2000), we investigated whether Na,K-ATPase activity was involved in the observed modulatory effects of $[K^+]_o$. The pump inhibitor ouabain (1 mM) was applied for 1 min before superfusing astrocytes with glutamate, which caused $[Na^+]_i$ to slowly rise (Fig. 3A). The addition of 200 μ M glutamate induced a sudden acceleration of the $[Na^+]_i$ rise that lasted until glutamate washout. Figure 3B shows that during Na,K-ATPase inhibition, the response slope was markedly larger in 3 versus 5.4 mM $[K^+]_o$. In a further analysis, the rate of $[Na^+]_i$ rise (i.e., local slope) was plotted against time (see Supplementary Fig. S4) and showed a significantly higher slope in the first minute of glutamate-induced Na^+ response for lower $[K^+]_o$. This analysis also showed that the decline of Na^+ influx rate, i.e., transporter deactivation (Chatton et al. 2000), occurred in both situations and tended to converge over time. Under our experimental conditions, the rodent Na,K-ATPase is rapidly and completely blocked by application of a high concentration of ouabain (1 mM) consistent with both experimental (O'Brien et al. 1994; Chatton et al. 2000, 2003) and modeling (Chatton et al. 2000) results. These experiments indicate that the effects of $[K^+]_o$ on the response to glutamate do not require Na,K-ATPase activity and point to an effect on glutamate transporter itself.

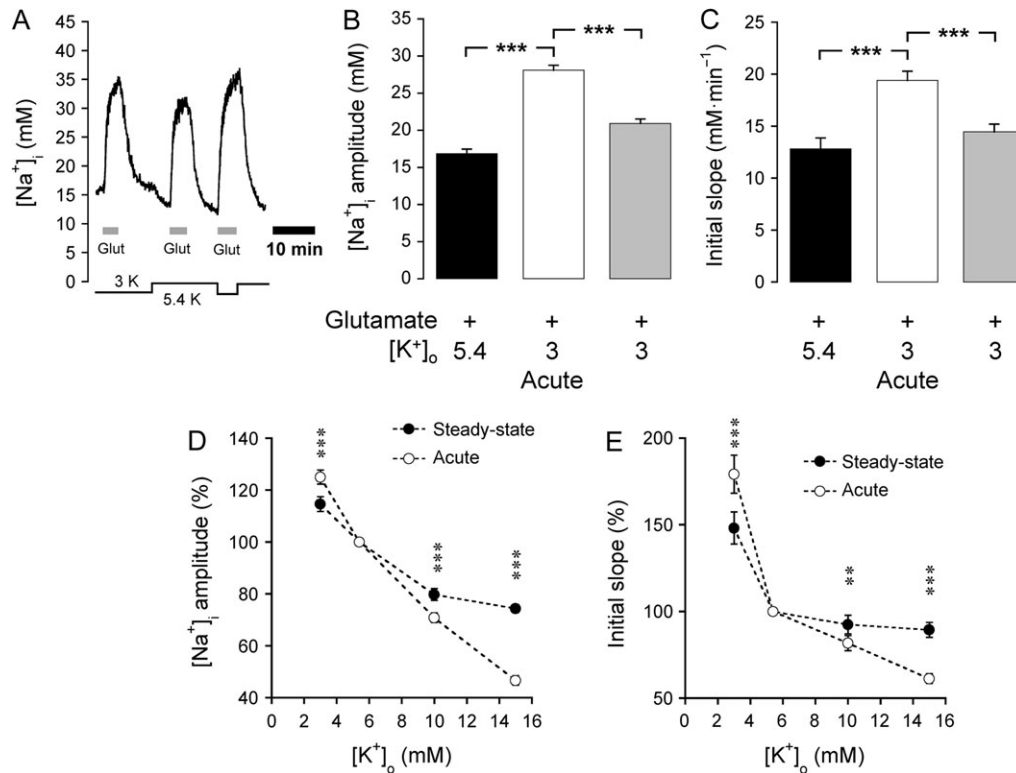


Figure 2. Acute effects of $[K^+]_o$ on the $[Na^+]_i$ response to glutamate. (A) Representative trace of intracellular Na^+ dynamics during $200 \mu M$ glutamate superfusion in 5.4 and 3 mM $[K^+]_o$ with and without equilibration period. Mean amplitudes (B) and initial rate of $[Na^+]_i$ rise (C) induced by glutamate in 5.4 mM $[K^+]_o$ (black bars) solutions compared with responses observed in 3 mM $[K^+]_o$ without (white bar) or with (gray bar) equilibration period ($n = 117$ cells, 12 exp). (D, E) Synchronized glutamate and high $[K^+]_o$ (open circles) led to a steeper modulation of the response amplitude (D) and initial rate of rise (E), in comparison with a steady-state situation (closed circles). (5.4 mM $[K^+]_o$: $n = 58$ cells, 6 exp; 10 mM $[K^+]_o$: $n = 90$ cells, 9 exp; 15 mM $[K^+]_o$: $n = 80$ cells, 8 exp).

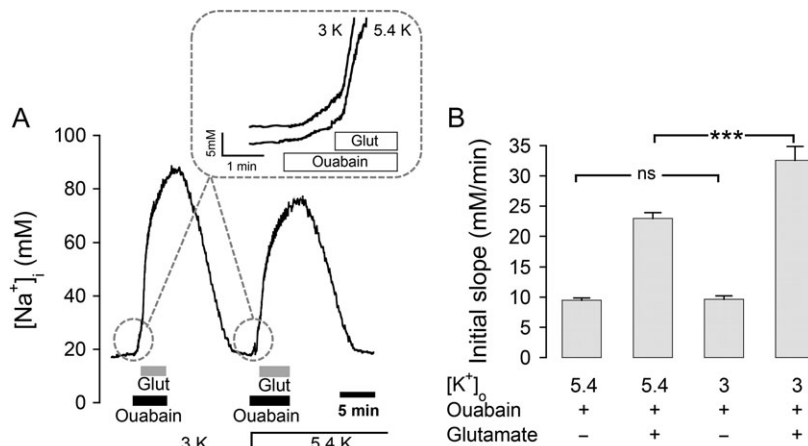


Figure 3. $[K^+]_o$ effects on glutamate-induced $[Na^+]_i$ response does not depend on the activity of the Na,K-ATPase. (A) Representative trace of $[Na^+]_i$ dynamics during $200 \mu M$ glutamate superfusion at 5.4 and 3 mM $[K^+]_o$ while blocking the Na,K-ATPase with 1 mM ouabain ($n = 65$ cells, 7 exp). The inset depicts the gradual $[Na^+]_i$ increase induced by ouabain alone, then its acceleration upon addition of glutamate. (B) The initial rate of $[Na^+]_i$ rise ($mM \cdot min^{-1}$) was calculated from the initial linear $[Na^+]_i$ rise following glutamate application ($n = 65$ cells, 7 exp).

$[K^+]_o$ Modulation of Glial Glutamate Transporter Currents in HEK-GLT-1 Cells are not Mediated by Changes in Membrane Potential (V_m)

The electrogenicity of glutamate transporters makes them sensitive to V_m (Huxley and Stampfli 1951). Under our experimental conditions, in acute cortical slices, we observed that

increasing the $[K^+]_o$ from 3 to 5.4 mM caused a 6.4 mV depolarization of the astrocyte membrane (data not shown). To investigate whether the voltage-dependence of glutamate transport might underlie the observed $[K^+]_o$ effects on the Na^+ response, the transporter current was assessed using whole-cell patch-clamp in HEK-GLT-1 cells clamped at -80 mV. Glutamate ($200 \mu M$) applications induced an inward current (Fig. 4A) that

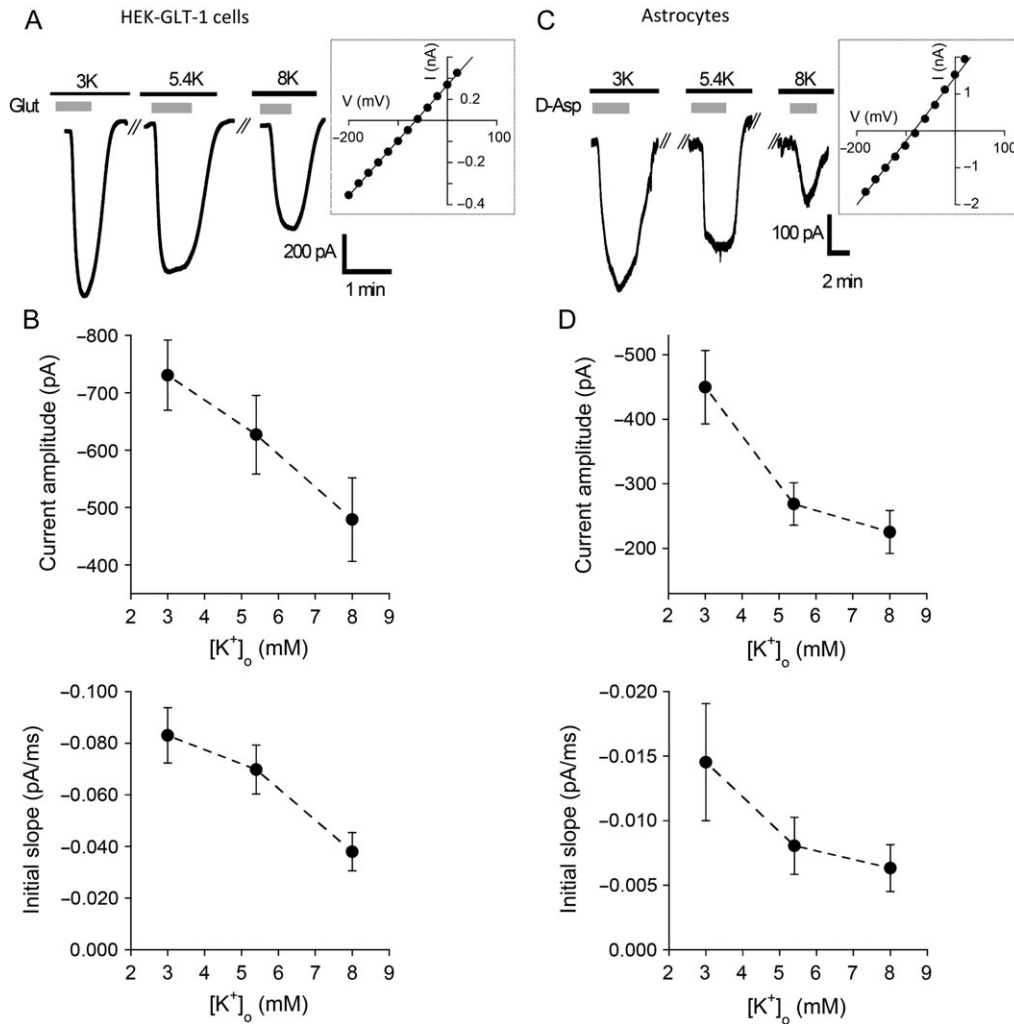


Figure 4. $[K^+]_o$ -modulation of the glutamate transporter current: electrophysiological responses of HEK-GLT-1 cells and astrocytes in acute slices in whole-cell voltage-clamp. (A) Modulation by $[K^+]_o$ of transporter current induced by $200\ \mu\text{M}$ glutamate superfusion of a HEK-GLT-1 cell. Inset: Corresponding current-voltage (I/V_m) relationship. (B) Modulation of slow inward current induced by D-Asp ($1\ \text{mM}$) on a passive astrocyte clamped at $-80\ \text{mV}$ in the brain slice under the influence of increasing $[K^+]_o$ superfusion. Inset: I/V_m relationship of the same astrocyte. (C, D) Mean values \pm SEM of maximum inward current amplitude (top) or initial slope (bottom) in HEK-GLT-1 cells ($n = 5$) or astrocytes ($n = 6$) plotted against $[K^+]_o$ in control condition.

was inhibited by bath application of the specific glutamate transporter inhibitor TFB-TBOA ($200\ \text{nM}$, see Supplementary Fig. S5) (Shimamoto et al. 2004; Bozzo and Chatton 2010). Both the amplitude and the time course of the glutamate associated current were decreased with rising $[K^+]_o$ from 3 to 8 mM (Fig. 4B). This observation, made at clamped voltage, confirms that the $[K^+]_o$ associated modulation of glutamate transport activity is not solely due to its effect on membrane potential.

$[K^+]_o$ Modulates Glial Glutamate Transporter Currents in Cortical Slices

We then investigated whether $[K^+]_o$ also affected astrocyte responses in situ. We recorded astrocytes of layer II/III mouse cortex in the whole-cell patch-clamp configuration. Astrocytes were clamped at $-80\ \text{mV}$ and membrane currents recorded (Fig. 4C). We found that bath application of D-Asp ($1\ \text{mM}$) in the presence of NMDAR antagonist D-AP5 caused a marked inward current that TFB-TBOA could inhibit by 81% (see Supplementary Fig. S5), confirming that glutamate transporters are responsible for the observed response induced by D-Asp. Figure 4D indicates

that the $[K^+]_o$ modulation of glutamate transporters is present in astrocytes in situ and can also be assessed by its associated transporter current.

Energy Metabolic Consequences of the $[K^+]_o$ Modulation of Glutamate Transport

Astrocytic energy demands are tightly coupled to the Na^+ load caused by glutamate uptake and the consecutive activation of the Na,K-ATPase (Magistretti et al. 1999; Magistretti and Chatton 2005). To assess how these energy demands are influenced by $[K^+]_o$, we monitored changes of intracellular free Mg^{2+} using the fluorescent probe MgG , as described before (Magistretti and Chatton 2005), as well as using the genetically encoded ATP sensor ATeam (Imamura et al. 2009). We found that $[K^+]_o$ increases alone decreased ATP hydrolysis (see Supplementary Fig. S6A,B), an observation compatible with Na,K-ATPase activity changes (Fig. 3). We then found that increasing $[K^+]_o$ negatively modulated both the amplitude of the ATP hydrolysis response (see Supplementary Fig. S6C,D) and the drop of cytosolic ATP levels (see Supplementary Fig. S6F,G)

caused by 200 μ M glutamate application. These measurements indicate that the inhibition of glutamate transporter activity observed in high $[K^+]_o$ is accompanied by lower rates of ATP hydrolysis, and hence lower energy demands.

Increasing $[K^+]_o$ Decreases mEPSCs Frequency in Acute Brain Slices

$[K^+]_o$ elevations of 3 mM from baseline are very likely to occur during non-pathological neuronal activity (Heinemann and Lux 1977). Such a change falls within the range of ~50% inhibition of the astrocytic glutamate transporter associated current according to our measurements (Fig. 4D). As an initial hypothesis, one could expect synaptic transmission to be potentiated in 6 versus 3 mM $[K^+]_o$ because of 1) the rise of extracellular glutamate concentrations due to weakened clearance efficacy, 2) the depolarizing effect on cell membrane potential associated with increased $[K^+]_o$. To test this hypothesis, we evaluated the outcome of changing $[K^+]_o$ from 3 to 6 mM on basal excitatory neurotransmission. Figure 5A shows electrophysiological traces of mEPSCs from representative neurons in layer II/III in acute cortical slices. The mean frequency of mEPSCs significantly decreased by 35% with the bath application of 6 mM $[K^+]_o$ (Fig. 5F) suggesting a depression of glutamate release with higher $[K^+]_o$. The mean amplitude or the kinetics of mEPSCs did not differ as illustrated by a corresponding superimposed averaged individual event trace (Fig. 5D,F). Representative cumulative percentile histograms (Fig. 5E) revealed the dramatically altered frequency distribution (K-S test, $z = 3.37$; $P < 0.001$, 6 mM $[K^+]_o$ vs. baseline) and the modest change in amplitude distribution ($z = 2.36$; $P < 0.001$). These findings indicate that increased $[K^+]_o$, which we showed to cause depression of glutamate uptake, did not enhance but rather dampened basal excitatory neurotransmission. We next investigated mechanisms that could underline this overall inhibitory activity associated with increased $[K^+]_o$.

The Inhibitory Effect of Increased $[K^+]_o$ on Excitatory Neurotransmission Requires mGluR_{2,3} Activation

Glutamate spillover occurring consecutively to pharmacological inhibition of glutamate transporters (Maki et al. 1994; Iserhot et al. 2004; Tsukada et al. 2005) or in a brain region with decreased glial coverage (Oliet et al. 2001) has been proposed to decrease glutamate release via presynaptic mGluR activation. The inhibitory effect of increased $[K^+]_o$ on glutamate transport could mobilize similar mechanisms. We targeted group II metabotropic receptors, associated with G_i proteins, known to decrease the probability of glutamate release upon activation. These receptors are expressed in the mouse neocortex (Reid and Romano 2001). Figure 5B shows the representative mEPSCs traces at 3 and 6 mM $[K^+]_o$ in the presence of LY341495 (50 nM), the specific and potent antagonist of group II mGluRs (Kingston et al. 1998) and the corresponding averaged individual event trace of mEPSCs (Fig. 5D, middle). LY341495 application itself had no significant effect on either frequency or amplitude (data not shown). However, in the presence of the mGluR_{2,3} blockade by LY341495, elevated $[K^+]_o$ failed to induce any changes in either mEPSC frequency or amplitude (Fig. 5F). These analyses confirm that the depression of excitatory synaptic activity exerted by an increased $[K^+]_o$ is blocked by mGluR_{2,3} activation.

$[K^+]_o$ Does Not Potentiate the Activation of NMDARs

Glutamate receptor-mediated mEPSCs were recorded at a holding voltage of -80 mV, which does not allow for investigating the post-synaptic NMDAR opening probability, which might be increased by $[K^+]_o$ -associated membrane depolarization. Depolarization has been indeed reported to alleviate the Mg^{2+} block from the NMDAR channel pore (Espinosa and Kavalali 2009). To investigate whether NMDAR activation was mediated by the change in membrane voltage associated with the increase in $[K^+]_o$, we repeated the previous experiment measuring mEPSCs. The NMDAR antagonist D-AP5 (50 μ M) was applied in addition to 6 mM $[K^+]_o$ (see representative traces in Fig. 5C). Electrophysiologically characterized cells were depolarized by -6.94 ± 1.51 mV ($P < 0.01$, $n = 6$, data not shown) in increased $[K^+]_o$ versus baseline condition. The changes in mEPSC frequency while applying 6 mM $[K^+]_o$ were similar to what found with the mEPSC recordings, i.e., a reduction of the frequency of events by one-third in 6 mM $[K^+]_o$ while the amplitude of these excitatory events was not significantly different from the baseline (Fig. 5D bottom). The presence of D-AP5 revealed a further decrease of the amplitude of events (-10%), but was not significant compared to the 6 mM $[K^+]_o$ condition. These data suggests that higher $[K^+]_o$ does not cause a significant activation of NMDAR located on either the pre- or post-synaptic sides (Fig. 5F).

$[K^+]_o$ Does Not Potentiate the Activation of Presynaptic Voltage Dependent Calcium Channels

K^+ -associated membrane depolarization could also modify glutamate neurotransmission from the presynaptic side via the presynaptic voltage dependent calcium (Ca_v) channels. To test this hypothesis, mEPSCs were recorded in the presence of the Ca_v blockers ω -agatoxin-TK (120 nM) and SNX-482 (60 nM), specific blockers of the presynaptic subtypes, the P/Q type $Ca_v2.1$ and R type $Ca_v2.3$, respectively (Teramoto et al. 1997; Newcomb et al. 1998). This set of experiments (see Supplementary Fig. S7) shows that the reduction of mEPSC frequency associated to elevated $[K^+]_o$ was not significantly more pronounced in presence of the Ca_v blockers.

$[K^+]_o$ and TFB-TBOA Share Inhibitory Actions on mEPSCs

The depression of mEPSCs frequency associated with increased $[K^+]_o$ was similar to the effects reported during pharmacological inhibition of the glutamate transporter (Maki et al. 1994; Oliet et al. 2001; Reid and Romano 2001; Iserhot et al. 2004), which was shown to be the consequence of extrasynaptic glutamate spillover and subsequent activation of presynaptic neuronal group II mGluRs. To our knowledge, such mechanisms have not been reported in the mouse neocortex where our studies were made. We therefore tested the outcome of pharmacological inhibition of glutamate transport on synaptic neurotransmission in this brain region. TFB-TBOA was applied in 3 mM $[K^+]_o$ at 80 nM, a concentration causing a ~40% inhibition of glutamate transporters (Bozzo and Chatton 2010), and we observed a $28.6 \pm 7.3\%$ ($P = 0.03$, $n = 4$) decrease in mEPSCs frequency with no change in amplitude, recapitulating observations made in other brain regions (data not shown). In another set of experiments ($n = 5$ cells), we compared the effects of TFB-TBOA in 3 versus 6 mM $[K^+]_o$. Figure 5G again shows a decrease in mEPSCs mean frequency—but not in amplitude—in the

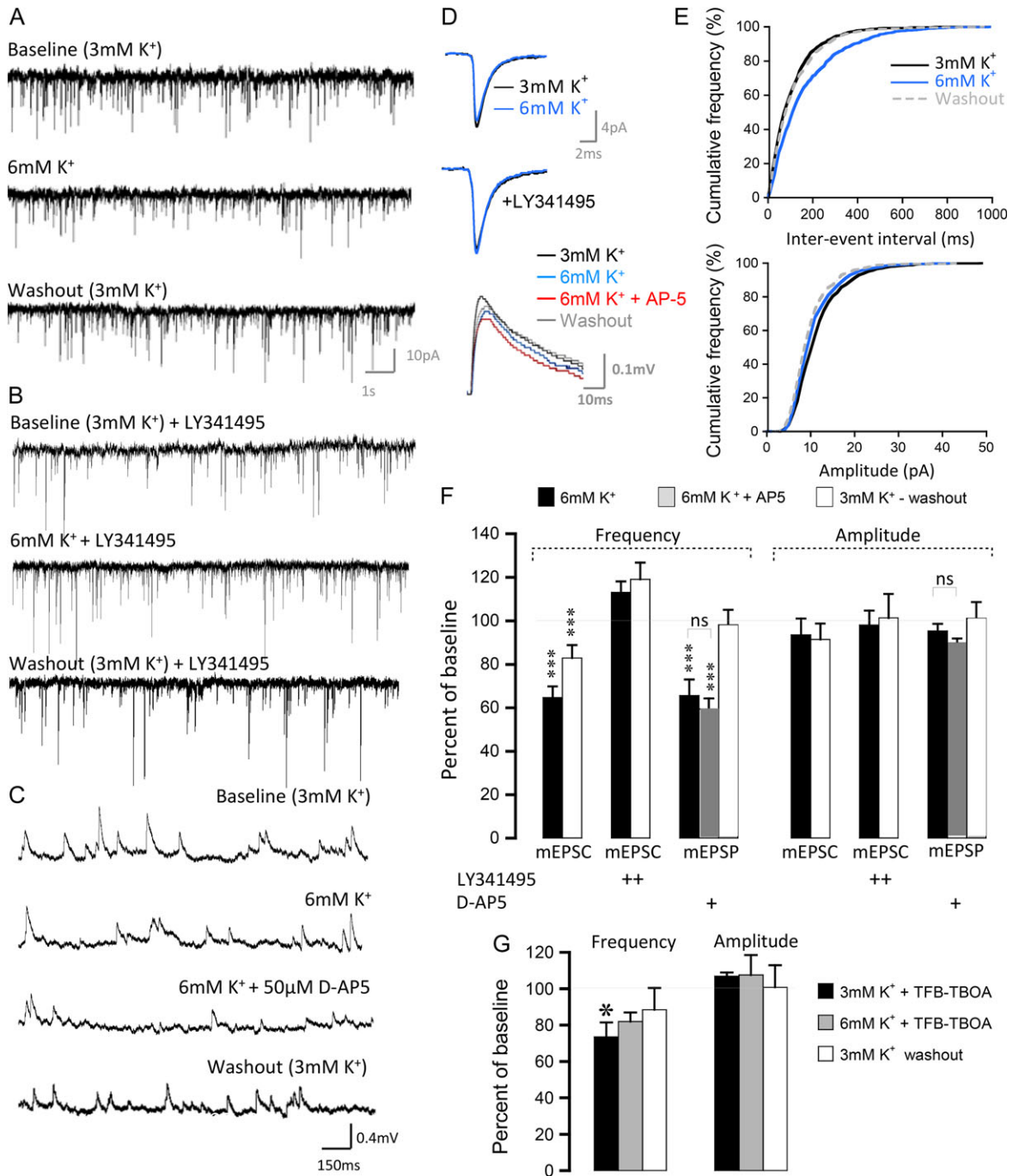


Figure 5. [K⁺]_o elevation decreases mEPSC frequency by a presynaptic mGluR II mechanism. (A–C) Representative mEPSCs (A, B) and mEPSPs (C) traces from cells recorded at 3 mM K control and washout (top, bottom), 6 mM [K⁺]_o alone or in the presence of antagonists for mGluR_{2,3} (LY341495, B) or for NMDA (AP5, C, middle). (D) Corresponding overlaid traces of mEPSC/PS averaged from the cells in A (top), B (middle) and C (bottom) demonstrating similar kinetics in 3 and 6 mM [K⁺]_o. (E) Cumulative probability distributions of mEPSC inter-event interval (top) and amplitude (bottom) from the same cell as in (A) during baseline (black line), 6 mM [K⁺]_o application (blue line) and washout (gray dashed line). (F) mEPSC/P frequency and amplitude (%) in response to elevated [K⁺]_o alone or in the presence of mGluR_{2,3} or NMDAR blockers. Statistical significance was calculated against baseline values unless otherwise stated. (G) Effects of TFB-TBOA and [K⁺]_o on synaptic transmission. A depression of mEPSC frequency but not amplitude is observed upon glutamate transporter inhibition by TFB-TBOA alone. It is not potentiated by the combined application of both TFB-TBOA and increased [K⁺]_o (n = 5).

presence of TFB-TBOA combined or not with increased [K⁺]_o. Thus, the extent of inhibition caused by TFB-TBOA is not additive to the one caused by 6 mM [K⁺]_o, suggesting that TFB-TBOA and elevated [K⁺]_o share a common mechanism of action. Therefore, [K⁺]_o may be considered the first physiological mediator of glutamate transporter inhibition.

Discussion

A remarkable finding of our study is that increased [K⁺]_o represents a prominent physiological inhibitor of glutamate uptake, which has unanticipated fundamental functional implications. While [K⁺]_o induced inhibition of glutamate transporters should

increase the glutamate concentration in the synaptic cleft, we observed it ultimately leads to the overall depression of mEPSC frequency, notably via a presynaptic mechanism involving the activation of mGluR_{2,3} metabotropic receptors.

[K⁺]_o Changes in the Brain

In vivo, [K⁺]_o levels have been shown to undergo substantial fluctuations during physiological and pathological conditions. During activity, repolarization of the neuronal membrane leads to an increase of [K⁺]_o in the proximity of active neurons, as well as in the surrounding network due to diffusion. Without adequate regulation, an accumulation of extracellular K⁺ would rapidly abolish electrical activity. Astrocytes are equipped with active and passive mechanisms for K⁺ uptake, such as inwardly rectifying K⁺ channels (Kir), Na⁺/K⁺/Cl⁻ cotransporters, and Na, K-ATPase. Astrocytes form a syncytium, and using these clearance mechanisms, they collectively perform rapid K⁺ redistribution in the brain (Kofuji and Newman 2004). Of particular note is the Kir4.1 channel, which is abundant in synaptic regions and perivascular endfeet (Higashi et al. 2001). Interestingly, it has been demonstrated that functional Kir4.1 expression is decreased in a mouse model of Huntington's disease (HD), which leads to striatal [K⁺]_o elevation (Tong et al. 2014). This could be reversed by viral delivery of Kir4.1 channels to striatal astrocytes. In addition, there are indications of interactions between the glutamate and K⁺ clearance mechanisms, as suggested by the demonstration of impaired glutamate uptake described in a Kir4.1 knock-out mouse model (Djukic et al. 2007).

While [K⁺]_o level is ~3 mM at rest, it may reach a concentration of ~12 mM during epileptiform activity (Kofuji and Newman 2004). Accordingly, our study investigated the cross-talk between glutamate transport and [K⁺]_o levels in the 3–15 mM range. The default concentrations of external potassium were set at different values in the in vitro versus ex vivo experiments. For primary astrocyte experiments, the default external K⁺ concentration was set to 5.4 mM in order to maintain the K⁺ concentration used in cell culture medium and prevent any initial K⁺ change. A 3 mM K⁺ concentration point was added to the set of cultured cells experiments as matter of comparison with the ex vivo acute slice experiments.

[K⁺]_o-Dependent Glutamate Transport Modulation

During activity, astrocyte processes surrounding synapses are exposed to both glutamate and K⁺, which are increased in the same time window. Glutamate is rapidly removed from the extracellular space both by Na⁺-coupled glutamate transporters, expressed at high density at the astrocyte membranes ensheathing the synaptic elements (Danbolt 2001), and by those present at the synaptic elements themselves (Rimmele and Rosenberg 2016).

The present study provides evidence for a K⁺-dependent modulation of glutamate uptake. For the same glutamate concentration applied, the amplitude of [Na⁺]_i response decreased by 3.5-fold within the range from 3 to 15 mM [K⁺]_o in situations of steady-state [K⁺]_o. Interestingly, when investigating the time dependency of the effect of [K⁺]_o on glutamate transport, we found that synchronized high [K⁺]_o and glutamate application led to a more pronounced reduction in the response compared to glutamate application in a steady-state condition. Such simultaneous and localized variations in both K⁺ and glutamate might be more reflective of what the membrane processes of

the astrocyte that tightly ensheathes synapses in vivo actually face. Given the immediacy of the responses we observed to [K⁺]_o changes, significant contribution of intracellular signaling pathways or biochemical processes such as phosphorylation or protein trafficking is unlikely. For example, cAMP production increases associated with K⁺ elevation requires a few minutes delay (Choi et al. 2012). Furthermore, the presence of bicarbonate is necessary for this cAMP rise to occur as it depends on the bicarbonate-dependent activation of soluble adenylylase. The [K⁺]_o-regulated uptake we report here is immediate and effective in bicarbonate-free solutions and is therefore unlikely to be associated with cAMP changes.

Several lines of evidence indicated that glutamate transporters are the prime target of this regulation by [K⁺]_o, as the same phenomenon was observed using the transporter substrate D-Asp both in primary cultures and in acute slices. Moreover, the [K⁺]_o effect persisted in the presence of ouabain, excluding a direct role of Na,K-ATPase, as could have been envisaged based on the reported physical and functional association between glutamate transporters and the pump (Cholet et al. 2002; Rose et al. 2009; Matos et al. 2013). In addition, as the glutamate transport cycle is electrogenic, variations of the membrane potential associated with [K⁺]_o changes could underlie the observed modulation. However, glutamate transport studied in voltage-clamp mode in HEK-GLT-1 cells or in astrocytes in acute brain slices exhibited the same [K⁺]_o modulation as in non-voltage clamped cells, consistent with a [K⁺]_o effect that is not entirely attributable to membrane potential changes.

Proposed Mechanism of the [K⁺]_o-Mediated Modulation of Transport

Glutamate transport has a complex stoichiometry of 3 Na⁺ and one H⁺ entering with glutamate in exchange for one K⁺ (Zerangue and Kavanaugh 1996). Transport steps occur in 2 half-cycles: first glutamate is co-transported with 3 Na⁺ ions and 1 H⁺ which is followed by a reorientation of the binding sites upon countertransport of K⁺ in a “ready for uptake” position, with the outward facing side (Kanner 2006). It has been proposed that an elevation of [K⁺]_o would increase the proportion of transporters in the inward-facing conformation and therefore limit the transport cycling rate (Kanner 2006). This is supported by experiments performed with brain plasma membrane saccules, where external K⁺ had an inhibitory effect on vesicle uptake of glutamate in the low millimolar range (Danbolt and Storm-Mathisen 1986), which also occurred in the presence of ionophores or in the absence of transmembrane ion gradients. This K⁺-mediated inhibition of glutamate uptake could therefore constitute the predominant mechanism underlying the [K⁺]_o modulation in the present study.

The structural basis for glutamate transport function is under thorough research, among which investigations focused on the K⁺ binding site. Targeted mutations in the K⁺ binding site preventing binding caused the abortion of the glutamate transport cycle of the mutated GLT-1 (Kavanaugh et al. 1997). These experiments suggest that interfering with the countertransport of K⁺ might impede the rate of glutamate transport. An additional model reviewed by Vandenberg and Ryan (2013) proposed that the glutamate transporter would be equipped with an additional K⁺ binding site that would overlap with that of glutamate. According to this latter hypothesis, the subsequent binding competition between glutamate and K⁺ would directly challenge glutamate uptake, especially in conditions of increased [K⁺]_o.

Functional Implications of [K⁺]_o Dependent Glutamate Uptake

This modulation of glutamate transport by [K⁺]_o has several important functional implications, considering the fluctuations of [K⁺]_o occurring during neuronal activity in both physiological and pathological conditions (for reviews, see [Kofuji and Newman 2004](#); [Sykova and Nicholson 2008](#)). An increase of +3 mM [K⁺]_o from basal [K⁺]_o leads to a reduction to 60% of glutamate transporter current in astrocytes. This novel K⁺-dependent regulation of the glutamate transporter could be proposed as a mechanistic hypothesis for the recent findings of [Armbruster et al. \(2016\)](#). This study shows, in cortical slices, a slowing down of glutamate uptake, assessed by an extracellular glutamate sensor that is dependent on the frequency and duration of neuronal activity rather than on the amount of glutamate released. In this context, [K⁺]_o, raising during sustained neuronal activity, possibly tunes down the glutamate uptake.

One could wonder what the functional advantage of such a modulation of glutamate transport by [K⁺]_o would be. At the bioenergetic level, Na⁺-coupled glutamate transport activity, tightly coupled with the Na,K-ATPase ([Magistretti and Chatton 2005](#)), comes with a substantial energy cost. An increase in [K⁺]_o is expected to decrease pump-associated cost by 2 mechanisms. 1) Baseline [Na⁺]_i in astrocytes is influenced by [K⁺]_o, as reported in the present study and previously ([Rose and Ransom 1996a](#); [Bittner et al. 2011](#)). [Na⁺]_i is lowered in high [K⁺]_o and energy measurements converge towards a decrease in ATP consumed by the Na,K-ATPase or an increased ATP/ADP ratio. 2) A [K⁺]_o-modulated decrease of glutamate uptake will cause a corresponding reduced Na,K-ATPase response, and associated ATP hydrolysis.

At the level of neuronal network activity, the pharmacological impairment of glutamate transporter activity is reported to favor glutamate accumulation and spillover ([Tsukada et al. 2005](#)). Accordingly, increased [K⁺]_o and its inhibitory action on glutamate transporters would also be very likely to lead to comparable glutamate accumulation in addition to cell membrane depolarization. Rather than potentiating synaptic glutamate transmission, we found that a moderate increase in [K⁺]_o caused a depression of excitatory presynaptic transmission via an indirect mechanism, involving a decrease in synaptic vesicle release probability. To test this hypothesis in our conditions, we applied LY341495, a potent antagonist of group II mGluR ([Kingston et al. 1998](#)), which completely abolished the depressive effect of increased [K⁺]_o on mEPSCs frequency. Our findings are consistent with previous studies employing a pharmacological inhibition of

glutamate uptake and reporting a depression of excitatory synaptic transmission due to the activation of group II mGluRs ([Maki et al. 1994](#); [Reid and Romano 2001](#); [Iserhot et al. 2004](#)). Group II mGluR encompasses mGluR_{2,3} which have been shown to be expressed in the adult mouse cerebral cortex ([Reid and Romano 2001](#); [Renger et al. 2002](#)), mainly at the neuronal presynaptic membrane ([jin et al. 2016](#)). These G_{β/γ} coupled receptors are reported to inhibit cAMP signaling and, downstream, neurotransmitter release ([Benneyworth et al. 2007](#)). While application of either 6 mM [K⁺]_o or TFB-TBOA, a potent inhibitor of glutamate transporters ([Shimamoto et al. 2004](#)), depressed mEPSCs frequency—but not amplitude—by about 30%, applying a combination of both 6 mM [K⁺]_o and TFB-TBOA did not cause an additional depression of mEPSCs. These non-additive effects indicate that pharmacological and K⁺-dependent inhibition of glutamate transport dampen excitatory presynaptic transmission through shared mechanisms. This negative feedback on excitatory neurotransmission elicited by increased extracellular potassium through scaling down of glutamate transport could be considered a plausible scenario in a situation where neuronal activity might be blocked. For example in the epilepsy study of [Bazzigaluppi et al. \(2016\)](#), K⁺ application alone in an in vivo mouse model did not trigger the seizures observed with the 4-aminopyridine application, although increased [K⁺]_o was of similar magnitude in both conditions.

Conclusion

We show that the glutamate concentration in the synaptic cleft does not only depend on calcium dependent release, but also on the [K⁺]_o-dependent control of glutamate uptake. These 2 parameters happen to be linked, as we unveiled a novel negative feedback cascade linking [K⁺]_o elevation, glutamate transporter inhibition, and presynaptic mGluR activation. This mechanism depicted in [Figure 6](#) could be fundamental for efficiently constraining excitatory neuronal activity in presence of raising [K⁺]_o, likely to occur during sustained neuronal activity. This study shows that the K⁺-coupling of glutamate transport represents a way of tuning synaptic transmission, not envisaged to date.

While the role of glutamate transporter in brain tissue is extensively studied—notably in the context of pathologies—it is with the general assumption that its transport capabilities are mainly determined by its level and pattern of expression. In this study, we unveil that these parameters are not the only determinants of glutamate uptake efficiency. [K⁺]_o is known to have a strong impact on neuronal excitability, and is also altered in several pathologies such as epilepsy ([Frohlich et al. 2008](#)) and HD ([Tong et al. 2014](#)). Now [K⁺]_o, as a physiological modulator of glutamate transport, must also be considered when studying glutamate transport efficiency. The subtle interplay between K⁺ and glutamate transport in both physiological and pathological conditions is of paramount importance and needs to be considered to better understand glutamate homeostasis.

Supplementary Material

Supplementary material are available at *Cerebral Cortex* online.

Funding

This work was supported by grant #31 003A-159513/1 from the Swiss National Science Foundation to J-Y Chatton.

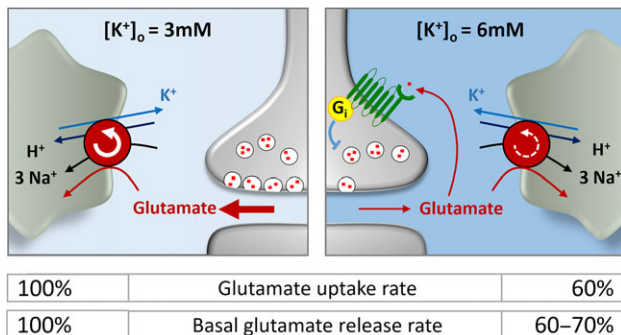


Figure 6. Summary scheme showing the new physiological roles of K⁺. This diagram depicts the impact [K⁺]_o changes have on synaptic neurotransmission through glutamate uptake inhibition and mGluR_{2,3} activation.

Notes

We thank Nicolas Demaurex and Hiroyuki Noji for providing us with the ATeam fluorescent construct, Marcus Rattray for providing a clone of HEK-GLT-1 cells, Anita Luthi for providing drugs, Rudy Kraftsik for advice on statistical analyses and Julien Puyal and collaborators for help with plasmid production. *Conflict of Interest*: None declared.

References

- Armbruster M, Hanson E, Dulla C. 2016. Glutamate clearance is locally modulated by presynaptic neuronal activity in the cerebral cortex. *J Neurosci*. 36:10404–10415.
- Barbour B, Keller BU, Llano I, Marty A. 1994. Prolonged presence of glutamate during excitatory synaptic transmission to cerebellar Purkinje cells. *Neuron*. 12:1331–1343.
- Bazzigaluppi P, Weisspapir I, Stefanovic B, Leybaert L, Carlen PL. 2016. Astrocytic gap junction blockade markedly increases extracellular potassium without causing seizures in the mouse neocortex. *Neurobiol Dis*. 101:1–7.
- Benneyworth MA, Xiang Z, Smith RL, Garcia EE, Conn PJ, Sanders-Bush E. 2007. A selective positive allosteric modulator of metabotropic glutamate receptor subtype 2 blocks a hallucinogenic drug model of psychosis. *Mol Pharmacol*. 72:477–484.
- Bergles DE, Jahr CE. 1997. Synaptic activation of glutamate transporters in hippocampal astrocytes. *Neuron*. 19:1297–1308.
- Bittner CX, Valdebenito R, Ruminot I, Loaiza A, Larenas V, Sotelo-Hitschfeld T, Moldenhauer H, San Martin A, Gutierrez R, Zambrano M, et al. 2011. Fast and reversible stimulation of astrocytic glycolysis by K^+ and a delayed and persistent effect of glutamate. *J Neurosci*. 31:4709–4713.
- Bozzo L, Chatton J-Y. 2010. Inhibitory effects of (2S, 3S)-3-[3-[4-(trifluoromethyl)benzoylamino]benzyloxy]aspartate (TFB-TBOA) on the astrocytic sodium responses to glutamate. *Brain Res*. 1316:27–34.
- Brew H, Attwell D. 1987. Electrogenic glutamate uptake is a major current carrier in the membrane of axolotl retinal glial cells. *Nature*. 327:707–709.
- Chatton J-Y, Marquet P, Magistretti PJ. 2000. A quantitative analysis of L-glutamate-regulated Na^+ dynamics in mouse cortical astrocytes: implications for cellular bioenergetics. *Eur J Neurosci*. 12:3843–3853.
- Chatton J-Y, Pellerin L, Magistretti PJ. 2003. GABA uptake into astrocytes is not associated with significant metabolic cost: implications for brain imaging of inhibitory transmission. *Proc Natl Acad Sci USA*. 100:12456–12461.
- Chesler M. 2003. Regulation and modulation of pH in the brain. *Physiol Rev*. 83:1183–1221.
- Choi HB, Gordon GR, Zhou N, Tai C, Rungta RL, Martinez J, Milner TA, Ryu JK, McLarnon JG, Tresguerres M, et al. 2012. Metabolic communication between astrocytes and neurons via bicarbonate-responsive soluble adenylyl cyclase. *Neuron*. 75:1094–1104.
- Cholet N, Pellerin L, Magistretti PJ, Hamel E. 2002. Similar perisynaptic glial localization for the Na^+, K^+ -ATPase alpha 2 subunit and the glutamate transporters GLAST and GLT-1 in the rat somatosensory cortex. *Cereb Cortex*. 12:515–525.
- Danbolt NC. 2001. Glutamate uptake. *Prog Neurobiol*. 65:1–105.
- Danbolt NC, Storm-Mathisen J. 1986. Inhibition by K^+ of Na^+ -dependent D-aspartate uptake into brain membrane saccules. *J Neurochem*. 47:825–830.
- Deitmer JW, Rose CR. 1996. pH regulation and proton signalling by glial cells. *Prog Neurobiol*. 48:73–103.
- Djukic B, Casper KB, Philpot BD, Chin LS, McCarthy KD. 2007. Conditional knock-out of Kir4.1 leads to glial membrane depolarization, inhibition of potassium and glutamate uptake, and enhanced short-term synaptic potentiation. *J Neurosci*. 27:11354–11365.
- Espinosa F, Kavalali ET. 2009. NMDA receptor activation by spontaneous glutamatergic neurotransmission. *J Neurophysiol*. 101:2290–2296.
- Frohlich F, Bazhenov M, Iragui-Madoz V, Sejnowski TJ. 2008. Potassium dynamics in the epileptic cortex: new insights on an old topic. *Neuroscientist*. 14:422–433.
- Heinemann U, Lux HD. 1977. Ceiling of stimulus induced rises in extracellular potassium concentration in the cerebral cortex of cat. *Brain Res*. 120:231–249.
- Higashi K, Fujita A, Inanobe A, Tanemoto M, Doi K, Kubo T, Kurachi Y. 2001. An inwardly rectifying $K(+) channel$, Kir4.1, expressed in astrocytes surrounds synapses and blood vessels in brain. *Am J Physiol Cell Physiol*. 281:C922–C931.
- Huxley AF, Stampfli R. 1951. Effect of potassium and sodium on resting and action potentials of single myelinated nerve fibers. *J Physiol (London)*. 112:496–508.
- Imamura H, Nhat KP, Togawa H, Saito K, Iino R, Kato-Yamada Y, Nagai T, Noji H. 2009. Visualization of ATP levels inside single living cells with fluorescence resonance energy transfer-based genetically encoded indicators. *Proc Natl Acad Sci USA*. 106:15651–15656.
- Iserhot C, Gebhardt C, Schmitz D, Heinemann U. 2004. Glutamate transporters and metabotropic receptors regulate excitatory neurotransmission in the medial entorhinal cortex of the rat. *Brain Res*. 1027:151–160.
- Jin LE, Wang M, Yang ST, Yang Y, Galvin VC, Lightbourne TC, Ottenheimer D, Zhong Q, Stein J, Raja A, et al. 2016. mGluR2/3 mechanisms in primate dorsolateral prefrontal cortex: evidence for both presynaptic and postsynaptic actions. *Mol Psychiatry*. doi:10.1038/mp.2016.1129.
- Kanner BI. 2006. Structure and function of sodium-coupled GABA and glutamate transporters. *J Membr Biol*. 213:89–100.
- Kavanaugh MP, Bendahan A, Zerangue N, Zhang Y, Kanner BI. 1997. Mutation of an amino acid residue influencing potassium coupling in the glutamate transporter GLT-1 induces obligate exchange. *J Biol Chem*. 272:1703–1708.
- Kingston AE, Ornstein PL, Wright RA, Johnson BG, Mayne NG, Burnett JP, Belagaje R, Wu S, Schoepp DD. 1998. LY341495 is a nanomolar potent and selective antagonist of group II metabotropic glutamate receptors. *Neuropharmacology*. 37:1–12.
- Kofuji P, Newman EA. 2004. Potassium buffering in the central nervous system. *Neuroscience*. 129:1045–1056.
- Lamy CM, Chatton JY. 2011. Optical probing of sodium dynamics in neurons and astrocytes. *NeuroImage*. 58:572–578.
- Levy LM, Warr O, Attwell D. 1998. Stoichiometry of the glial glutamate transporter GLT-1 expressed inducibly in a Chinese hamster ovary cell line selected for low endogenous Na^+ -dependent glutamate uptake. *J Neurosci*. 18:9620–9628.
- Magistretti PJ, Chatton J-Y. 2005. Relationship between L-glutamate-regulated intracellular Na^+ dynamics and ATP hydrolysis in astrocytes. *J Neural Transm*. 112:77–85.
- Magistretti PJ, Pellerin L, Rothman DL, Shulman RG. 1999. Energy on demand. *Science*. 283:496–497.
- Maki R, Robinson MB, Dichter MA. 1994. The glutamate uptake inhibitor L-trans-pyrrolidine-2,4-dicarboxylate depresses excitatory synaptic transmission via a presynaptic

- mechanism in cultured hippocampal neurons. *J Neurosci.* 14:6754–6762.
- Matos M, Augusto E, Agostinho P, Cunha RA, Chen JF. 2013. Antagonistic interaction between adenosine A_{2A} receptors and Na⁺/K⁺-ATPase- α 2 controlling glutamate uptake in astrocytes. *J Neurosci.* 33:18492–18502.
- Newcomb R, Szoke B, Palma A, Wang G, Chen X, Hopkins W, Cong R, Miller J, Urge L, Tarczy-Hornoch K, et al. 1998. Selective peptide antagonist of the class E calcium channel from the venom of the tarantula *Hysterocrates gigas*. *Biochemistry.* 37:15353–15362.
- O'Brien WJ, Lingrel JB, Wallick ET. 1994. Ouabain binding kinetics of the rat alpha two and alpha three isoforms of the sodium-potassium adenosine triphosphate. *Arch Biochem Biophys.* 310:32–39.
- Oliet SH, Piet R, Poulain DA. 2001. Control of glutamate clearance and synaptic efficacy by glial coverage of neurons. *Science.* 292:923–926.
- Reid SN, Romano C. 2001. Developmental and sensory-dependent changes of group II metabotropic glutamate receptors. *J Comp Neurol.* 429:270–276.
- Renger JJ, Hartman KN, Tsuchimoto Y, Yokoi M, Nakanishi S, Hensch TK. 2002. Experience-dependent plasticity without long-term depression by type 2 metabotropic glutamate receptors in developing visual cortex. *Proc Natl Acad Sci USA.* 99:1041–1046.
- Rimmele TS, Rosenberg PA. 2016. GLT-1: The elusive presynaptic glutamate transporter. *Neurochem Int.* 98:19–28.
- Rose CR, Ransom BR. 1996a. Intracellular sodium homeostasis in rat hippocampal astrocytes. *J Physiol (London).* 491:291–305.
- Rose CR, Ransom BR. 1996b. Mechanisms of H⁺ and Na⁺ changes induced by glutamate, kainate, and D-aspartate in rat hippocampal astrocytes. *J Neurosci.* 16:5393–5404.
- Rose EM, Koo JC, Antflick JE, Ahmed SM, Angers S, Hampson DR. 2009. Glutamate transporter coupling to Na,K-ATPase. *J Neurosci.* 29:8143–8155.
- Rossi DJ, Oshima T, Attwell D. 2000. Glutamate release in severe brain ischaemia is mainly by reversed uptake. *Nature.* 403:316–321.
- Rothstein JD, Martin L, Levey AI, Dykes-Hoberg M, Jin L, Wu D, Nash N, Kuncl RW. 1994. Localization of neuronal and glial glutamate transporters. *Neuron.* 13:713–725.
- Ruminot I, Gutierrez R, Pena-Munzenmayer G, Anazco C, Sotelo-Hitschfeld T, Lerchundi R, Niemeyer MI, Shull GE, Barros LF. 2011. NBCe1 mediates the acute stimulation of astrocytic glycolysis by extracellular K⁺. *J Neurosci.* 31:14264–14271.
- Schmitt BM, Berger UV, Douglas RM, Bevenssee MO, Hediger MA, Haddad GG, Boron WF. 2000. Na/HCO₃ cotransporters in rat brain: expression in glia, neurons, and choroid plexus. *J Neurosci.* 20:6839–6848.
- Shih PY, Savtchenko LP, Kamasawa N, Dembitskaya Y, McHugh TJ, Rusakov DA, Shigemoto R, Semyanov A. 2013. Retrograde synaptic signaling mediated by K⁺ efflux through postsynaptic NMDA receptors. *Cell Rep.* 5:941–951.
- Shimamoto K, Sakai R, Takaoka K, Yumoto N, Nakajima T, Amara SG, Shigeri Y. 2004. Characterization of novel L-threo-beta-benzoyloxyaspartate derivatives, potent blockers of the glutamate transporters. *Mol Pharmacol.* 65:1008–1015.
- Slotboom DJ, Konings WN, Lolkema JS. 1999. Structural features of the glutamate transporter family. *Microbiol Mol Biol Rev.* 63:293–307.
- Sorg O, Magistretti PJ. 1992. Vasoactive intestinal peptide and noradrenaline exert long-term control on glycogen levels in astrocytes: blockade by protein synthesis inhibition. *J Neurosci.* 12:4923–4931.
- Sykova E, Nicholson C. 2008. Diffusion in brain extracellular space. *Physiol Rev.* 88:1277–1340.
- Szatkowski M, Barbour B, Attwell D. 1990. Non-vesicular release of glutamate from glial cells by reversed electrogenic glutamate uptake. *Nature.* 348:443–446.
- Teramoto T, Niidome T, Kimura M, Ohgoh M, Nishizawa Y, Katayama K, Mayumi T, Sawada K. 1997. A novel type of calcium channel sensitive to omega-agatoxin-TK in cultured rat cerebral cortical neurons. *Brain Res.* 756:225–230.
- Tong X, Ao Y, Faas GC, Nwaobi SE, Xu J, Hausteine MD, Anderson MA, Mody I, Olsen ML, Sofroniew MV, et al. 2014. Astrocyte Kir4.1 ion channel deficits contribute to neuronal dysfunction in Huntington's disease model mice. *Nat Neurosci.* 17:694–703.
- Tsukada S, Iino M, Takayasu Y, Shimamoto K, Ozawa S. 2005. Effects of a novel glutamate transporter blocker, (2S, 3S)-3-[3-[4-(trifluoromethyl)benzoylamino]benzyloxy]aspartate (TFB-TBOA), on activities of hippocampal neurons. *Neuropharmacology.* 48:479–491.
- Vandenberg RJ, Ryan RM. 2013. Mechanisms of glutamate transport. *Physiol Rev.* 93:1621–1657.
- Zerangue N, Kavanaugh MP. 1996. Flux coupling in a neuronal glutamate transporter. *Nature.* 383:634–637.